Environmentally Influenced Fatigue Crack Path in Titanium Alloys

C. Sarrazin-Baudoux

Laboratoire de Mécanique et de Physique des Matériaux, UMR CNRS 6617,
ENSMA, Poitiers/Futuroscope, France, baudoux@lmpm.ensma.fr

ABSTRACT. *This paper is focused on the effect of environment on the fatigue crack path on two titanium alloys used in aeronautical turbine engines at high temperatures. The objective is to try to put in light the crack propagation mechanisms involved through microscopic observations on the crack path and fracture surface. A Ti-6A-4V alloy for turbine disks is studied at 300°C in three microstrutural states and a Ti6246 alloy for turbine disks and blades is used for tests at 500°C, this last alloy being dedicated to operate at higher temperature. Tests were run in laboratory air, in high vacuum and in other environments with controlled partial pressure of water vapor and oxygen permitting to distinguish the intrinsic behavior from the effects related to the environment, the temperature, the stress level which can act separately or simultaneously. It is shown on this study that the crack path and the fracture surface morphology are strongly dependent on the cracking process involved.*

INTRODUCTION

Titanium alloys are interesting to several industrial applications including transportation and biotechnology, aerospace designers having been particularly interested because of the combination of their fatigue and time-dependent mechanical properties, good formability, high specific properties due to a relatively low density, and high resistance to aggressive environmental and impact loads. The improvement of the engine performance being directly related to the increase of the operating temperature, Ti-rich Ti-Al alloys (Al < 12.4 wt %) which account for this goal are the most critically studied. These alloys are used under cyclic loading conditions in aggressive environments such as ambient air at elevated temperature, and can be submitted to the superposition of constant loading and large number of small amplitude perturbations. Then a detailed characterization of these alloys is required in order to ensure good damage tolerance properties for their operational life. The present paper is addressing a study of the near-threshold fatigue crack propagation behavior of two titanium alloys type Ti-6Al-4V and Ti6246. It is particularly focused on the relation existing between the crack path and the fatigue crack growth mechanisms in accordance with the microstructure and with respect to the loading conditions, the temperature and the gaseous environment.

EXPERIMENTALS

Two materials were used in this investigation: i) a forged $\alpha+\beta$ Ti-6Al-4V alloy heat treated for 1 hour at 965°C, water quenched, and aged in three different conditions to obtain the microstructures presented in Fig. 1, ii) a α/β Ti6246 which forms Widmanstätten microstructure consisting of 75% of α platelets contained in prior β grains with size around 300 μm.

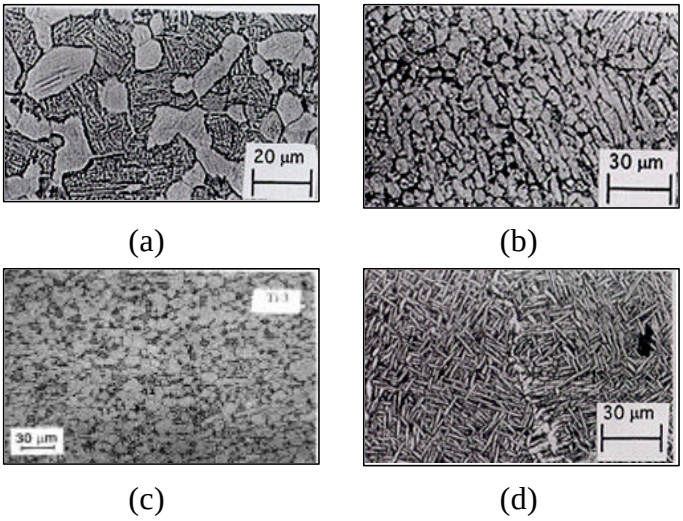

Figure 1. Microstructures of the Ti-6Al-4V alloy : a) bimodal with 40% equiaxed α_p, Ti1, b) heterogeneous with 80% of coarse lamellar or globular α_p, Ti2, c) homogeneous with70% fine globular α_p, Ti3 and d) Ti6246 : 75 % α_p Windmanstätten intermeshed.

Tests were conducted on compact tension specimen (10 mm thick and 40 mm wide) on a servo-hydraulic machine at temperatures up to 500°C under sinusoidal load time waveform at a frequency of 35 Hz. Tests under controlled gaseous atmospheres and under high vacuum were performed in an environmental chamber. A recording electrical potential system was used for monitoring crack length. Crack tip opening measurements were made by mean of a capacitive detector for tests at R=0.1. Some other tests were performed at constant K_{max}, the R ratio being increased when ΔK was decreased so as to avoid crack closure using the differential procedure proposed by Kikukawa and al. [1].

INFLUENCE OF MICROSTRUCTURE AND ENVIRONMENT ON FCP IN A Ti6Al4V ALLOY at 300°C.

Intrinsic Behavior

In order to separate the respective influence of the microstructure and of the environment, the intrinsic near-threshold propagation curves were determined in high vacuum at constant K_{max} (i.e. in condition without closure) for the three different aged

conditions of the Ti-6Al-4V (Fig. 2). For crack growth rates higher than 10^{-8} m/cycle (mid-rate range), the curves appear independent of the microstructure.

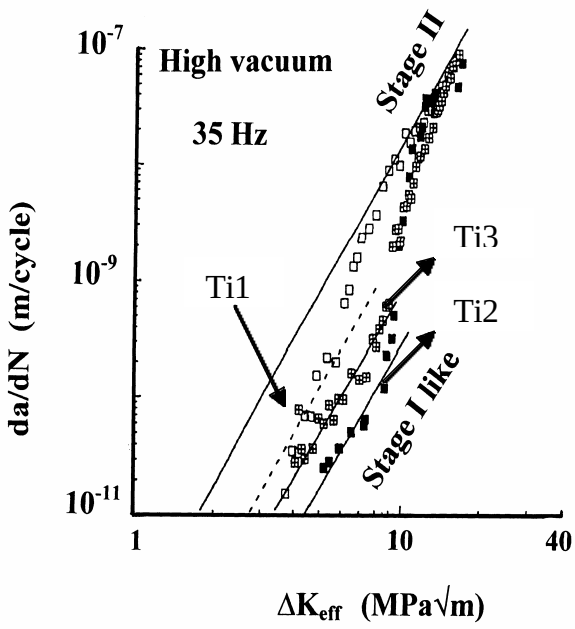

Figure 2. Near-threshold fatigue crack propagation in high vacuum for the three microstructures of the Ti-6Al-4V alloy (Ti1, Ti2 and Ti3).

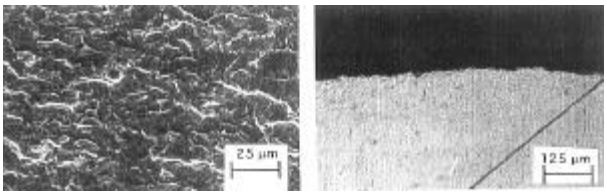

(a) (b)

Figure 3. Stage II crack propagation path in the mid-rate range in the Ti2 alloy: a) microfractographic aspect of the fracture surface, b) crack profile.

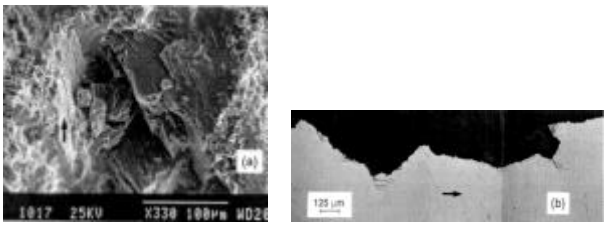

(a) (b)

Figure 4. Stage I like crack propagation path in the near-threshold domain on the Ti2 microstructure a) microfractographic aspect of the fracture surface, b) crack profile.

In all case a stage II propagation is operative with a uniform transgranular morphology as illustrated in Fig. 3. This change in the crack propagation behavior can be attributed to a fundamental change in the crack growth mechanism from a stage II propagation in the mid-rate range to a very slow crystallographic propagation called "stage I- like" in the near-threshold area. It is not really a stage I crack, because if at the scale of each individual grain this mechanism corresponds to a stage I propagation, it must be notice that at macroscopic scale, the crack remains normal to the stress axis as a stage II crack. An identification of the involved crystallographic planes have been made by means of the technique of Electron Back Scattering Diffusion [3]. The corresponding channeling patterns are illustrated with related pole figures in Fig. 5 and support that all facets orientation lies within the basal planes of the α phase. The intrinsic stage II

regime for all metallic alloys [2] has been described by the following relation derived from the initial models of Weertman and Rice [4,5] :

$$da/dN = A/D^* (\Delta Keff/E)^4 \quad (1)$$

with A dimensionless and D* a critical cumulative displacement as introduced by Weertman [6] or Rice [5]. This regime is mostly independent on the microstructure.

A best fit for the data representative of the intrinsic stage I-like propagation curves on the assumption of a slope m=4 is presented. The slower growth rate of this crystallographic regime can be analyzed as a lowering of ΔK_{eff} induced by crack branching and deflection, as proposed by Suresh [6], or by grain boundary barrier effect which is substantially enhanced when a single slip mechanism is operative.

The retardation effect is accentuated by coarse microstructure and high volume fraction of α_p. Thus, the stage I-like regime cannot be rationalized using a unique relation.

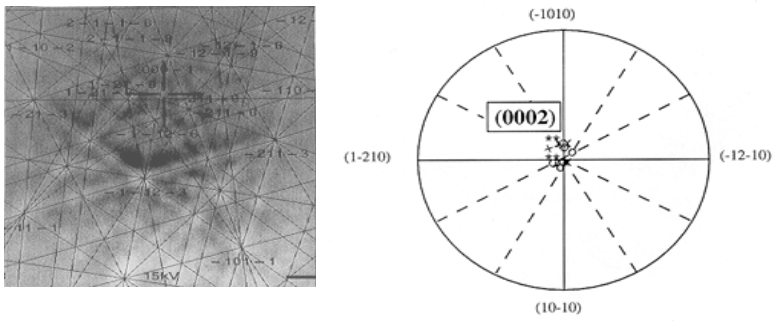

Figure 5. EBSD patterns on α laths of the Stage I like near-threshold crack surface of the Ti2 microstructure.

Environmentally Assisted Propagation

Figure 6 shows effective data obtained in ambient air, in high vacuum and other selected environments on the Ti2 microstructure. This diagram illustrates the specific influence of environment which clearly appears deleterious at low rates ($<<10^{-8}$ m/cycle). For growth rates higher than 10^{-8} m/cycle there is only a limited influence of environment on the crack propagation rates. But at lower growth rates the influence of environment becomes huge, the effective threshold in air being less than half than the threshold in vacuum (for threshold evaluated at 10^{-10} m/cycle) and the growth rates in air can be 100 time faster than in vacuum. The near threshold crack path in air and in high vacuum are very different. In air a stage II mechanism prevails while in vacuum a strong localization of the deformation within each individual a grain generate the highly crystallographic crack path illustrated and discussed in the previous section (Fig. 4).

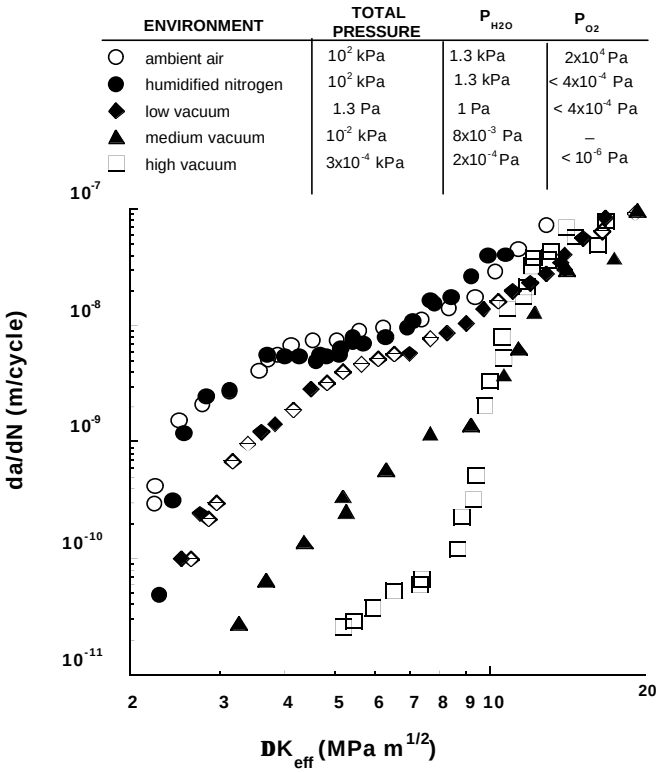

Figure 6. Effective crack propagation on the Ti2 type alloy under different selected environments including laboratory air and high vacuum at 300°C.

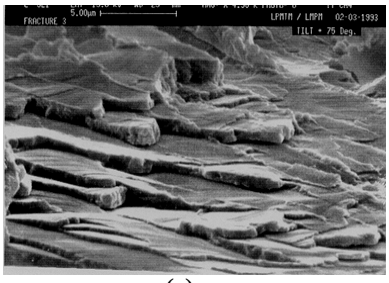

(a)

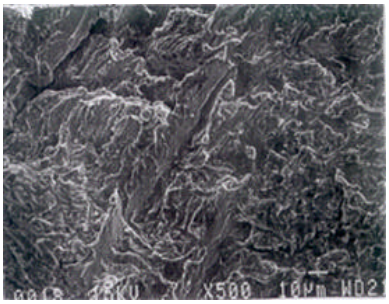

(b)

Figure 7. Near threshold cracked surfaces obtained on the ti2 alloy at 300°C showing to crack mechanism change from high vacuum (a) to medium vacuum (b).

An analysis of the residual gas using a mass spectrometer indicates 75% of water vapor in medium vacuum and an amount of oxygen lower than the resolution of measurement(<< 10^{-5} Pa).Then the dominant detrimental effect of water vapor is clearly demonstrated. This result indicates that even a very limited number of adsorbed water vapor molecules can modify the slip conditions and favor activation of some secondary slip systems generating a faster propagation regime close to the stage II regime. The cracked surfaces still present localized crystallographic areas (Fig. 7b) but globally the fracture surface is flatter and smoother than under high vacuum. When the partial pressure of water vapor is much higher (from 1 Pa to 1.3 kPa), the characteristic plateau range observed in active environments becomes progressively more and more pronounced, until it reaches a level and a shape similar to that observed in ambient air

or humidified nitrogen (1.3 kPa) without noticeable change in the transgranular stage II crack path.

COUPLED EFFECT OF LOADING CONDITION AND ENVIRONMENT ON FCP AT 500°C IN Ti6246 ALLOY

Figure 8 compares the da/dN-ΔK data of constant K_{max} threshold tests conducted at 500°C in air, high vacuum and humidified Argon at different K_{max} levels. Microfractographies of crack profiles and fracture surfaces corresponding to the different experimental conditions are also shown in this figure.

In high vacuum, no K_{max} effect is observed and the propagation curves are similar with a threshold ranging about 3 MPa√m. An illustration of the cracked surface obtained in the low ΔK range is given on the Fig. 8c showing a transgranular propagation with a highly strained β phase due to the great K_{max} levels.

In ambient air, for K_{max} ranging up to 55 MPa√m, crack growth rates are comparable, and hence independent on K_{max}. A substantial effect of environment is observed especially in the low ΔK range with rates of two orders of magnitude higher than those in high vacuum (at ΔK=3.5 MPa√m, da/dN =10^{-10} m/cycle in vacuum and 10^{-8} m/cycle in air), and a much lower threshold value close to 2 MPa√m. Such enhancement of the propagation in air at 500°C has been related to an environmental effect very much more pronounced at elevated temperature than at room temperature [7]. Nevertheless, the cracked surface in the near threshold (Fig. 8f) remains very similar to that obtained in vacuum.

At K_{max} of 57 MPa√m a steady crack growth regime is observed with a growth rate ranging about 3 to 4x10^{-9} m/cycle. Such a behavior is consistent with the superposition of fatigue and creep mechanisms. A comparable behavior is observed in air and in humidified Argon for ΔK above 2 MPa√m. But for lower ΔK range, a steady crack growth at about 2x10^{-9} m/cycle is detected in moist Argon at a critical K_{max} level which is only of 22 MPa√m. It is of importance to notice that the partial pressure of water vapor in the argon gas filling the chamber is comparable to that of laboratory air. So, the same amount of water vapor in a neutral gas appears to be much more detrimental than in air.

This would support that oxygen contained in air is more preventing the detrimental effect of water vapor than being detrimental gaseous specie. Such behavior in humidified Argon is associated to a mechanism different from the creep process operating in air and has been related to a stress corrosion cracking mechanism induced by water vapor. In air, the cracked surface and the crack path (Figs 8d and 8e) are mainly flat without secondary cracking, while in the argon (Fig. 8a) the crack profile is very tortuous with the presence of numerous secondary cracks and related branching supporting a huge embrittlement induced by water vapor [8,9]. The cracked surface corresponding to stress corrosion cracking process (Fig. 8b) shows very rough areas with intergranular decohesion at the prior-β grains which might be in accordance with a

strong embrittlement of grain boundaries by water vapor which is not observed in air (i.e. in presence of oxygen).

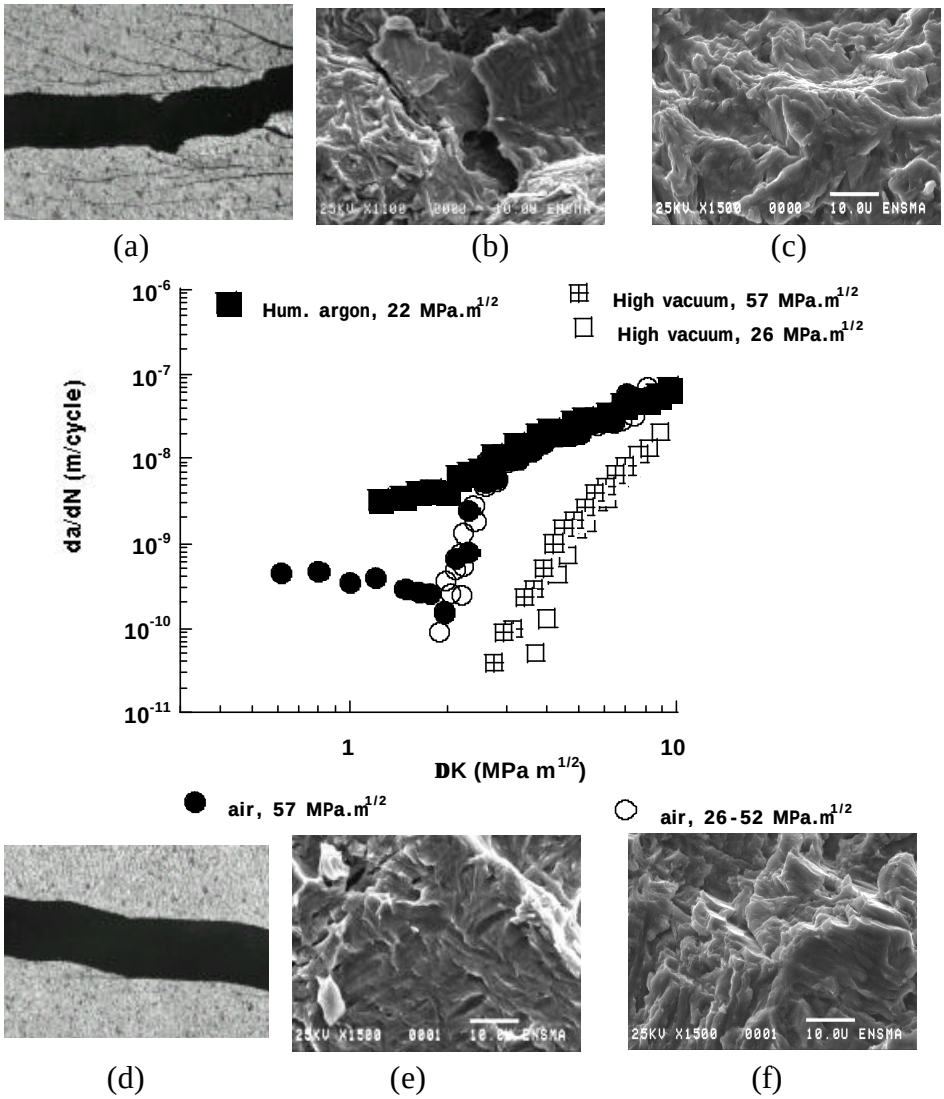

Figure 8. Influence of environment in the near threshold behavior at 500°C (35 Hz). a,b: hum. argon at K_{max} = 22 MPa m, c: high vacuum at K_{max} = 52 MPa m, d,e: ambient air at K_{max} = 57 MPa m, f: ambient air at K_{max} = 52 MPa m.

CONCLUSION

The near threshold crack path in titanium alloys at moderate and high temperature is very sensitive to environment, microstructure and their coupled effect. Three main

regimes are identified (Fig. 9): i) transgranular stage II, poorly affected by the microstructure, ii) transgranular stage I like, favored by aligned α lamellar colonies, iii) intergranular corrosion cracking, which follows boundaries of ex β grains.

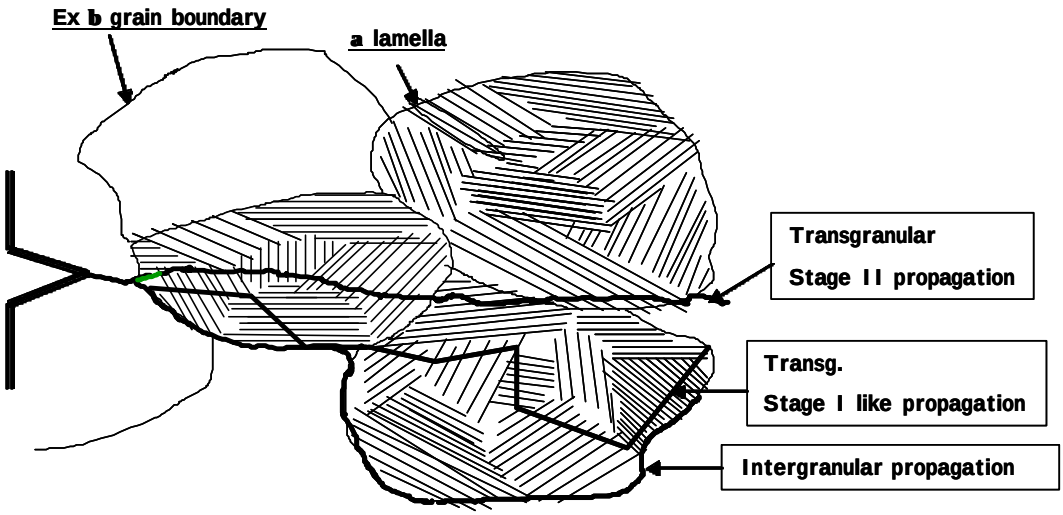

Figure 9. Schematic illustration of the three main propagation paths.

REFERENCES

1. Kikukawa, M., Jono, M. and Mikami, S. (1982) *J. Soc. Mat. Sci*. **31**, 438-487.
2. Petit, J., Henaff, G. and Sarrazin-Baudoux, C. (2000) In *Fatigue Crack Growth threshold , Endurance Limits, and Design, ASTM STP 1372*, pp.3-30, Newman, J. C. and Piascik, R. S., (Eds).
3. Sarrazin, C., Chiron, R., Lesterlin, S. and Petit, J. (1994) *Fat. Fract. Engng. Mat. and Struct*. **17,** 1383-1389.
4. Weertman, J. (1967) *International Journal of Fracture Mechanics* **2**, 460-467.
5. Rice, J.R. (1968) In: *Fracture*, pp.191-311, Liebowitz, H. (Ed.), Academic Press, New York.
6. Suresh, S., Zamishi, G.F. and Ritchie, R.O. (1981) *Met. Trans. A* **12**, 1435.
7. Sarrazin, C., Lesterlin, S. and Petit, J. (1996) European structural integrity society, *Proc. of the 11th European Conference on Fracture - ECF 11*, Poitiers, Mechanisms and mechanics of damage and failure, Ed. J. Petit, EMAS pub,UK, Vol. 2, pp.1249-1254
8. Mankowski, G. (1990) *Corrosion sous contrainte-Phénoménologies et mécanismes, Les éditions de physique*, Eds. D. Desjardins and R. Oltra, pp.645-684.
9. Dickson, J.I., Li, S.Q. and Baï lon, J.P. (1990) Aspects fractographiques de la corrosion sous contrainte. *Corrosion sous contrainte-Phénoménologies et mécanismes, Les éditions de physique*, Eds D. Desjardins and R. Oltra, pp.425-464.